

Immunopathology and Infectious Diseases

Therapeutic Effect of Melatonin in Experimental Uveitis

Pablo Horacio Sande,* Diego Carlos Fernandez,*
Hernán Javier Aldana Marcos,[†]
Mónica Silvia Chianelli,* Julieta Aisemberg,[‡]
Dafne Magalí Silberman,* Daniel Alberto Sáenz,*
and Ruth Estela Rosenstein*

From the Laboratorio de Neuroquímica Retiniana y Oftalmología Experimental, Departamento de Bioquímica Humana, Universidad de Buenos Aires, Centro de Estudios Farmacológicos y Botánicos Consejo Nacional de Investigaciones Científicas y Técnicas, Buenos Aires, Argentina, Laboratorio de Histología,[†] Facultad de Medicina, Universidad de Morón, Buenos Aires, Argentina, Laboratorio de Fisiopatología de la Preñez,[‡] Centro de Estudios Farmacológicos y Botánicos/Consejo Nacional de Investigaciones Científicas y Técnicas Buenos Aires, Argentina*

Uveitis is a common ophthalmic disorder that can be induced in hamsters by a single intravitreal injection of bacterial lipopolysaccharide (LPS). To examine the therapeutic effects of melatonin on uveitis, a pellet of melatonin was implanted subcutaneously 2 hours before the intravitreal injection of either vehicle or LPS. Both 24 hours and 8 days after the injection, inflammatory responses were evaluated in terms of i) the integrity of the blood-ocular barrier, ii) clinical signs, iii) histopathological studies, and iv) retinal function. Melatonin reduced the leakage of proteins and cells in the anterior segment of LPS-injected eyes, decreased clinical signs such as dilation of the iris and conjunctival vessels, and flare in the anterior chamber, and protected the ultrastructure of the blood-ocular barrier. A remarkable disorganization of rod outer segment membranous disks was observed in animals injected with LPS, whereas no morphological changes in photoreceptor outer segments were observed in animals treated with melatonin. Furthermore, melatonin prevented a decrease in LPS-induced electroretinographic activity. In addition, melatonin significantly abrogated the LPS-induced increase in retinal nitric-oxide synthase activity, tumor necrosis factor- α , and nuclear factor κ B p50 and p65 subunit levels. These results indicate that melatonin prevents the clinical, biochemical, histological, ultrastructural, and functional consequences of experimental uveitis, likely

through a nuclear factor κ B-dependent mechanism, and support the use of melatonin as a new therapeutic strategy for the treatment of uveitis. (Am J Pathol 2008; 173:1702–1713; DOI: 10.2353/ajpath.2008.080518)

Uveitis is a frequent ophthalmic disorder characterized by an acute, recurrent, or persistent ocular inflammation with disruption of the blood-ocular barrier (BOB), accompanied by protein leakage and leukocyte infiltration into the aqueous humor. Despite the fact that uveitis is one of the main causes of eye morbidity and loss of visual functions, the complexity of the biochemical and immune mechanisms involved in its generation and development remain unknown. Several lines of evidence support that the disease is due to damage generated by infiltrated leukocytes, which release cytokines^{1,2} and other inflammatory chemical mediators, like arachidonic acid metabolites,³ reactive oxygen species,^{4,5} and nitric oxide (NO),⁶ among many others. Arachidonic acid metabolites regulate vascular permeability, chemotaxis, and contribute to uveitis amplification.^{7,8} In addition, activated phagocytes synthesize large amounts of NO through a reaction catalyzed by the inducible isoform of NO synthase (iNOS).^{9,10} At present, the therapy for uveitis, generally based on the use of corticoids, is essentially directed toward pain reduction and avoiding lesions of ocular tissues.^{11,12} However, the immunosuppressive effect of corticoids may contribute to the development of the systemic disease, and their chronic use could induce cortisonic glaucoma.^{13,14} Non-steroidal anti-inflammatory drugs are also indicated for uveitis treatment, but they may delay the reparation process and coagulation, or produce acute renal insufficiency, gastrointestinal hemorrhage, or ulceration.^{15,16}

Supported by grants from the Agencia Nacional de Promoción Científica y Tecnológica (ANPCyT), the University of Buenos Aires, CONICET, Argentina, and the John Simon Guggenheim Memorial Foundation.

P.H.S. and D.C.F. contributed equally to this work.

Accepted for publication September 9, 2008.

Address reprint requests to Dr. Ruth E. Rosenstein, Departamento de Bioquímica Humana, Facultad de Medicina, CEFyBO, UBA. Paraguay 2155, 5°P, (1121), Buenos Aires, Argentina. E-mail: ruth@fmed.uba.ar.

Endotoxin-induced uveitis (EIU), a widely recognized experimental model for uveitis,¹⁷ is induced by the administration of bacterial lipopolysaccharide (LPS), a component of Gram-negative bacterial outer membranes. LPS enhances the expression of various inflammatory mediators, such as tumor necrosis factor (TNF)- α ,¹ interleukin (IL)-6,^{1,2} prostaglandin E₂,³ and NO.^{6,18} all of which contribute to the development of the disease. Several lines of evidence support that EIU mimics central features of human uveitis, such as the breakdown of the BOB, and infiltration of leukocytes. Although EIU was originally used as a model of anterior uveitis, increasing evidence shows that it also involves inflammation of the ocular posterior segment with recruitment of leukocytes that adhere to the retinal vasculature and infiltrate the vitreous cavity.¹⁹

Melatonin (5-methoxy-*N*-acetyltryptamine) is an endogenous neuromodulator in the retina of vertebrates.^{20–22} We have demonstrated that mean hamster retinal melatonin levels significantly increase after pinealectomy, supporting that in the golden hamster as in other species, retinal melatonin is generated within the tissue itself.²³ In contrast to the hormone of pineal origin, which is secreted to the body fluids, retinal melatonin is thought to act locally within the eye.²⁴ It was demonstrated that melatonin has an important immunomodulatory role and it may provide neuroprotection in different systems.²⁵ Although the full range of physiological actions of melatonin is still not completely known, it has been demonstrated that melatonin possesses widespread free radical scavenging and antioxidant activities,^{26,27} and that some of its scavenging actions are likely due to its metabolites, cyclic 3-hydroxymelatonin, N1-acetyl-N2-formyl-5-methoxykynuramine, and *N*-acetyl-5-methoxykynuramine.^{28,29} Several lines of evidence suggest that melatonin may act as a protective agent in ocular conditions such as photokeratitis, cataract, glaucoma, retinopathy of prematurity, and ischemia/reperfusion injury (for a review see ³⁰). Besides its antioxidant effect, several other mechanisms are considered to be involved in neuroprotection induced by melatonin, including its interaction with calmodulin³¹ and microtubular components,³² blockade of intracellular Ca²⁺ levels increase,³³ inhibition of the nitridergic pathway,^{34,35} decrease in vascular endothelial growth factor levels,^{36,37} and decrease in retinal glutamate synaptic concentrations,³⁸ among others. In this context, the aim of the present work was to analyze the therapeutic effect of melatonin in the golden hamster EIU.

Materials and Methods

Reagents and Drugs

All reagents were obtained from Sigma Chemical Co. (St. Louis, MO).

Animals

Male Syrian hamsters (average weight 120 \pm 20 g), derived from a stock supplied by Charles River Breeding Laboratories (Wilmington, MA), were kept under a 14

hours light: 10 hours dark lighting schedule (lights on at 0600 hours), with free access to food and water. All of the experiments were conducted in accordance with the Association for Research in Vision and Ophthalmology Statement for the Use of Animals in Ophthalmic and Vision Research. Intravitreal injections, implantation of the pellet of melatonin, as well as sacrifice of animals, were performed between 10 a.m. and 12 p.m.

Induction of Experimental Uveitis

Hamsters were anesthetized with ketamine hydrochloride (150 mg/kg) and xylazine hydrochloride (2 mg/kg) by i.p. administration. A drop of proparacaine (0.5%) was administered in each eye for local anesthesia. With a Hamilton syringe and a 30-gauge needle, 2 μ l of LPS from *Salmonella typhimurium* (0.5 mg/ml in sterile pyrogen-free saline) was injected into one eye of anesthetized hamsters, while an equal volume of vehicle (sterile pyrogen-free saline solution) was injected in the fellow eye. Injections were applied at 1 mm of the limbus, and the needle was left in the eye for 60 seconds to allow aqueous humor to flow out; this small volume prevented the increase in intraocular pressure and volume loss. One group of hamsters was subcutaneously implanted with a single pellet of melatonin (5 mg with 3% w/v vegetable oil) compressed in a cylinder of 2.5 mm diameter and 1 mm length), while a control group was sham-operated without pellet implanting. Vehicle or LPS were intravitreally injected 2 hours later.

Clinical Score

Six different parameters were considered when examining hamster eyes 24 hours after the intravitreal injection of vehicle or LPS in the presence or absence of melatonin. Clinical severity of these signs was graded on a scale from 0 to 16, as follows: degree of conjunctival (0 to 3) and episcleral hyperemia (0 to 3), degree of cornea inflammation (0 to 3), degree of alteration of iris and pupil (vasodilatation, synechia, presence of exudates at the pupil rim, and degree of miosis) (0 to 3). The absence (0) or presence of a cataract was scored 1 or 2 (less or more than 50% of the lens surface, respectively), whereas the degree of opacity of the posterior segment was scored 0 to 2. The animals were examined by a masked observer in a random order.

Integrity of the BOB

Aqueous Humor Samples

Animals were euthanized and the aqueous humor was collected immediately from each eye by anterior chamber puncture using a 30-gauge needle under a surgical microscope. Cell count and protein concentration in aqueous humor samples obtained 24 hours after the injection of vehicle or LPS were assayed to assess BOB integrity. The number of cells was manually counted using a Neubauer hemocytometer, and the number of cells

per μl was obtained by averaging the results of four fields from each sample.

Protein concentration in aqueous humor was determined by the method of Lowry et al³⁹ using bovine serum albumin as standard. Aqueous humor samples were stored on ice until testing, and cell counts and protein concentration were measured on the day of sample collection.

Lanthanum Tracer Studies

After anesthesia and thoracotomy, animals were perfused through the left ventricle with three perfusates, according to the method of DePace et al.⁴⁰ The initial perfusate was 10 to 15 ml of 1% NaNO_3 in normal saline. This was immediately followed by a 10-minute infusion with 50 to 100 ml of ionic lanthanum solution composed of 20 mmol/L $\text{La}(\text{NO}_3)_3 \cdot 6\text{H}_2\text{O}$, 80 mmol/L NaCl , 3.5 mmol/L KCl , 1.0 mmol/L CaCl_2 , 1.0 mmol/L MgCl_2 , and 1.0 mmol/L glucose, pH 7.4. Lanthanum nitrate solution was followed by an additional 10-minute perfusion with 50 to 100 ml of 2% glutaraldehyde and 2% paraformaldehyde prepared in a sulfate-salt solution containing 43 mmol/L Na_2SO_4 , 16 mmol/L NaHCO_3 , 10 mmol/L sodium acetate, 3.5 mmol/L KCl , 1.0 mmol/L CaCl_2 , 1.0 mmol/L MgCl_2 , 1.0 mmol/L glucose, 1.6 mmol/L Na_2HPO_4 , 0.4 mmol/L NaH_2PO_4 , and 33 mmol/L sucrose at pH 7.4. $\text{La}_2(\text{SO}_4)_3$ is insoluble, and electron dense precipitates facilitate ultrastructural localization of lanthanum. After perfusion, the retina was dissected out and after several washings, and tissue blocks were postfixed in 1% aqueous osmium tetroxide for 1 hour and processed for electron microscopy.

Histological Examination

Light Microscopy

Hamsters were euthanized 24 hours or 8 days after vehicle or LPS injection. Eyes were immediately enucleated and stored in phosphate-buffered saline containing 4% formaldehyde for 24 to 48 hours. Eyecups were then dehydrated, embedded in paraffin, and sectioned with a microtome at 5- μm thickness. The nictitans membrane was maintained in each eye to facilitate orientation. Each section was cut along the vertical meridian of the eye through the optic nerve head. In all cases microscopic images were digitally captured with a Nikon Eclipse E400 microscope (illumination: 6-V halogen lamp, 20W, equipped with a stabilized light source) via a Sony SSC-DC50 camera. The microscope was set up for Koehler illumination. The camera output was digitized into a 520 \times 390 pixel matrix (each pixel with 0 to 255 gray levels) with a Leadteck WinView 601 video capture card, displayed on a computer monitor, and saved as an image of 24 bit RGB in BMP format. For morphometric image processing, digitalized captured images were transferred to Scion Image for Windows analysis system (Scion Corporation β 4.0.2). Sections were stained with H&E and observed by a masked pathologist. Thickness of the ganglion cell layer, inner plexiform layer, inner

nuclear layer, outer plexiform layer, outer nuclear layer, and outer and inner photoreceptor segments were measured for each eye in micrometers in the same topographic region of retina. Six measurements (magnification = original \times 400) were obtained at 0.5 mm dorsal and ventral from the optic disk and averaged for each eye.

The number of neutrophils and macrophages located at both plexiform layers, and in inner and outer photoreceptor segments, was quantified. These layers were chosen for quantification due to the absence of neuronal and glial nuclei that could interfere with morphological identification of infiltrated cells. In six sections of whole retina for each eye, the total number of infiltrated cells and the proportion of neutrophils/macrophages were analyzed and expressed in number of infiltrated cells/100 μm of retina (magnification = original \times 400).

Immunohistochemistry

Antigen retrieval was performed by heating (90°C) for 30 minutes unstained paraffin sections immersed in citrate buffer, pH 6. For immunodetection of glial cells, sections were incubated overnight at 4°C with a mouse monoclonal anti-vimentin (clone V9, 1:100; DAKO, CA) or with a mouse monoclonal anti-glial fibrillary acidic protein (GFAP; 1:400; Sigma Chemical Co., St. Louis, MO). A labeled streptavidin-biotin immunohistochemical staining was performed using the LSAB2 System HRP Dakocyto-mation, according to manufacturer's instructions. Some sections were treated without the primary antibodies to confirm the specificity of immunoreactivity. To determine Müller cell density, the number of vimentin-labeled Müller cells in the inner plexiform layer was counted. Four measurements (magnification = original \times 400) were obtained at a 0.5 and 1.5 mm dorsal and ventral from the optic disk and averaged for each eye. The measurements were expressed in cells/100 μm of retina.

Electron Microscopy

For electron microscopy studies, tissue samples were fixed in 2% glutaraldehyde in 0.1 mol/L sodium phosphate buffer (pH 7.2) for 24 hours. Then, tissues were postfixed with 2% osmium tetroxide in sodium phosphate buffer. Dehydration was accomplished by gradual ethanol series and tissue samples were embedded in epoxy resin. Semithin sections were stained with toluidine blue and ultrathin sections were stained with uranyl acetate and lead citrate. Afterward, sections were viewed and photographed using a Zeiss M-109 Turbo transmission electron microscope.

Electroretinography

Electroretinographic activity was assessed in dark-adapted hamsters as previously described.⁴¹ After 6 hours of dark adaptation, hamsters were anesthetized with ketamine and xylazine under dim red illumination. Phenylephrine hydrochloride (2.5%) and 1% tropicamide (Alcon Laboratories, Buenos Aires, Argentina) were used

to dilate the pupils, and the cornea was intermittently irrigated with balanced salt solution (Alcon Laboratories, Buenos Aires, Argentina) to maintain the baseline recording and to prevent keratopathy. Hamsters were placed in a Ganzfeld light stimulator. All recordings were completed within 20 minutes of the induction of anesthesia and animals were kept warm during and after the procedure. A reference needle electrode was placed through the ear, a grounding electrode was attached to the back of the head, and a gold ring-shaped electrode was placed in contact with the central cornea. A 15-W red light was used to enable accurate electrode placement. This maneuver did not significantly affect dark adaptation and the red light was switched off during the recordings. Electroretinograms (ERGs) were recorded from both eyes simultaneously and the response to one flash of unattenuated white light (4 ms) from a photic stimulator set at maximum brightness (350 cd s/m² without filter) was amplified (gain set at 100), filtered (1.5-Hz low-pass filter, 1000 Hz high-pass filter), notch activated, and registered with an Akonic BIO-PC device (Akonic, Buenos Aires, Argentina). Each recording presented was the response to a single flash, and started simultaneously with the application of the stimulus. The a-wave amplitude was measured as the difference between the recording at onset and the trough of the negative deflection, whereas the b-wave amplitude was measured from the trough of the a-wave to the peak of the b-wave. The latencies of the a- and b-waves were measured as the time from stimulus onset to the maximum negative (a-wave), or positive (b-wave) deflections. The mean latencies and peak-to-peak amplitudes of the responses from each group of hamsters were compared. ERGs were performed 8 days after the injection of LPS or vehicle and they were assessed by operators who were blind with respect to the treatment applied to each eye.

NOS Activity Assessment

Animals were sacrificed by decapitation 24 hours after vehicle or LPS injections, and NOS activity was assessed as previously described.³⁴ Briefly, each retina was homogenized in 100 μ l of buffer solution containing 0.32 mol/L sucrose and 0.1 mmol/L EDTA, pH 7.4. Reaction mixtures contained 50 μ l of the enzyme source and 50 μ l of a buffer stock solution (final concentrations: 10 mmol/L HEPES, 3 mmol/L CaCl₂, 1 mmol/L NADPH, 5 μ M FAD, 1 mmol/L β -mercaptoethanol, L-³H-arginine, [5 μ Ci/ml, purity greater than 98%], and 1 μ M L-arginine). After incubation at 37°C for 30 minutes, the reaction was stopped by adding 200 μ l of buffer containing 50 mmol/L HEPES, 10 mmol/L EDTA, and 10 mmol/L EGTA, pH 5.5, and cooling the tubes for 5 minutes. The solution was mixed with 600 μ l of resin Dowex AG50W-X8 (Na⁺ form) to remove L-arginine, and centrifuged at 10,000 \times g for 5 minutes. L-³H-citrulline in the supernatant was quantified by liquid scintillation counting. Nonenzymatic conversion of L-³H-arginine to L-³H-citrulline was tested by adding buffer instead of the enzyme source.

Enzyme-Linked Immunosorbent Assay for TNF α

Each retina was homogenized in 150 μ l of buffer containing 20 mmol/L imidazole hydrochloride, 100 mmol/L KCl, 1 mmol/L MgCl₂, 1 mmol/L EGTA, 1% Triton, 10 mmol/L NaF, 1 mmol/L sodium molybdate, and 1 mmol/L EDTA supplemented with a cocktail of protease inhibitors before use. Samples were cleared by centrifugation for 10 minutes at 13,000 rpm. TNF α levels were estimated with enzyme-linked immunosorbent assay kits (TNF [Mono/Mono] Set of BD Biosciences Pharmingen, San Diego, CA), according to the manufacturer's instructions. The reaction was stopped and absorption was measured in an enzyme-linked immunosorbent assay reader at 450 nm. All measurements were performed in duplicate.

Western Blot Analysis for p65 and p50 Subunit of Nuclear Factor- κ B

Animals were sacrificed 3 hours after vehicle or LPS injection in the presence or absence of melatonin. Retinas (two per condition) were homogenized in 200 μ l of buffer A (10 mmol/L HEPES; pH 7.9, 1 mmol/L EDTA, 1 mmol/L EGTA, 10 mmol/L KCl, 1 mmol/L dithiothreitol, supplemented with a cocktail of protease inhibitors. After 15 minutes at 4°C, the tubes were gently vortexed for 15 seconds, and nuclei were collected by centrifugation at 8000 \times g for 15 minutes. The pellets were resuspended in 70 μ l buffer A supplemented with 20% (v/v) glycerol and 0.4 mol/L KCl, and mixed for 30 minutes at 4°C. Nuclear proteins were obtained by centrifugation at 13,000 rpm for 15 minutes, and aliquots of the supernatant (nuclear extracts) were stored at -80°C. For Western blot analysis, samples were boiled in Laemmli sample buffer, and equal amounts of protein (50 μ g) were separated by 10% SDS-polyacrylamide gel electrophoresis. Polyclonal antibodies specific for p65 and p50 subunit of NF κ B (1:500; Santa Cruz), were used for immunodetection. Anti- β -actin was used as control of equal loading and transfer efficiency. Band intensities were measured on a densitometric scanner (Amersham) and expressed in arbitrary units. Equal loading and transfer was ensured by reprobing the membranes for β -actin.

Melatonin Assessment

Retinal melatonin levels were assessed as previously described²³ in non-implanted animals (control), or 24 hours and 8 days after the implantation of a melatonin pellet. Briefly, retinas were homogenized in 2 ml of 0.1 mol/L HCl, and melatonin was extracted from the whole homogenate with 5 ml of dichloromethane. The organic phase was washed twice with 2% NaHCO₃ and distilled water. Aliquots of 1.5 ml of the organic layer were dried under vacuum and stored at -20°C until the radioimmunoassay was performed. The samples were resuspended in 100 μ l of buffer (6 mmol/L NaN₃, 0.1 mol/L KH₂PO₄, and 0.1% gelatin, pH 7.5) and then mixed with ³H-melatonin (20,000 to 24,000 dpm, specific activity 38.8 Ci/mmol) and 50 μ l of a melatonin antiserum kindly provided

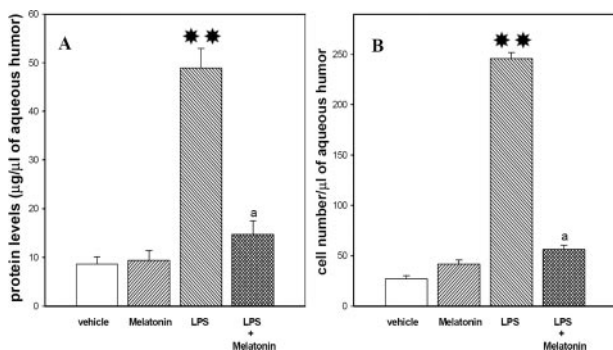


Figure 1. Effect of LPS on protein concentration and cell number in aqueous humor from golden hamster eyes, 24 hours after injection. Both parameters were significantly higher in LPS- than in vehicle-injected eyes. Melatonin significantly reduced protein concentrations (**panel A**) and cell number (**panel B**) in the aqueous humor from LPS-injected eyes. Data are mean \pm SE ($n = 10$ eyes per group), ** $P < 0.01$ vs. vehicle- injected eyes; a: $P < 0.01$ vs LPS-injected eyes by Tukey's test.

by Dr. Takashi Matozaki (Laboratory of Biosignal Sciences, Institute for Molecular and Cellular Regulation, Gunma University, Japan). The mixture was incubated for 2 hours at 37°C. The bound/free separation was performed by the dextrancharcoal method, and the radioactivity of supernatant was measured by a liquid scintillation counter. Melatonin values were obtained from a melatonin standard curve, with an assay limit sensitivity of 20 pg per tube.

Statistical Analysis

Statistical analysis of results was made by a two-way analysis of variance followed by a Tukey's test, or by a Mann-Whitney U -test, as stated.

Results

Figure 1 shows protein concentration and infiltrated cell count in the aqueous humor from eyes injected with vehicle or LPS in the presence or absence of a subcuta-

neous pellet of melatonin. Twenty four hours after the injection of LPS, increased amounts of proteins and cells were detected in the aqueous humor (Figure 1, A and B, respectively). Histological examination showed a high number of neutrophils in vitreous humor and retina at 24 hours postinjection of LPS, whereas mainly macrophages laying over the retinal pigment epithelium (RPE) were present 8 days after endotoxin injection (data not shown). Melatonin significantly reduced the content of proteins and cell number in eyes injected with LPS.

Signs of uveitis, such as dilation of the iris and conjunctival vessels, and flare in the anterior chamber, were observed 24 hours after the intravitreal injection of LPS. The clinical score of vehicle- or LPS-injected eyes, as well as representative images of golden hamster eyes injected with LPS or vehicle in the presence or absence of melatonin are shown in Figure 2. The treatment with melatonin significantly decreased the clinical score of LPS-injected eyes.

One day after the injection of LPS, the histological analysis revealed severe inflammatory signs affecting the iris-ciliary body, limbus, vitreous humor, and retina, showing massive inflammatory cell infiltration (Figure 3, A and F) as compared with vehicle (Figure 3D). In a later phase (8 days postinjection of LPS), the inflammation decreased (Figure 3C) but disorganization of photoreceptor outer segments persisted (Figure 3I). In these eyes, retinal detachments and loss of photoreceptors were observed (Figure 3K). In animals treated with melatonin, a significant reduction in the number of inflammatory cells infiltrating the eye was observed (Figure 3B and G). After 24 hours of injection, the mean thickness of the retina and all retinal layers was significantly higher in eyes injected with LPS than in vehicle-injected eyes, whereas the thickness of the retina and retinal layers from eyes injected with LPS and supplied with melatonin was significantly lower than in LPS-injected eyes (Table 1, Figure 3G). After 8 days, an LPS-induced thickness increase persisted only in the photoreceptor layer, which was also prevented by melatonin (Table 1, Figure 3, H-J).

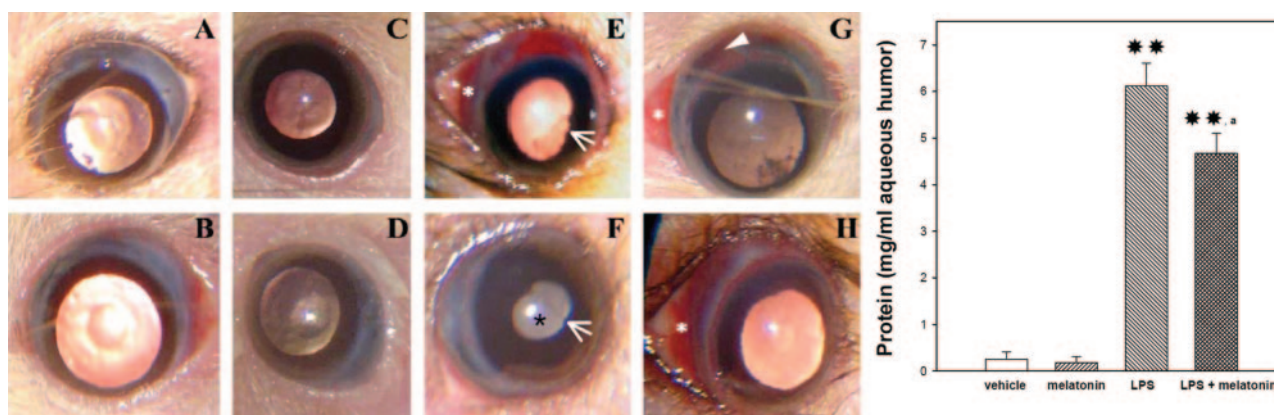


Figure 2. Left panel: Representative photographs of 2 eyes/group injected with vehicle or LPS in the presence or absence of melatonin, as follows: vehicle (A, B); melatonin (C, D); LPS (E, F); LPS + melatonin (G, H). Note the following clinical signs: white asterisk: conjunctival hyperemia; black asterisk: cataract; arrow: synechiae, and arrowhead: episcleral hyperemia. Right panel: Clinical score of hamster eyes injected with vehicle or LPS in the presence or absence of melatonin. After 24 hours of intravitreal injections, LPS significantly increased the clinical score, whereas the presence of melatonin significantly reduced the effect of LPS. Data are mean \pm SE ($n = 15$ eyes per group), ** $P < 0.01$ vs. vehicle injected eyes; a: $P < 0.01$ vs. LPS-injected eyes by Mann-Whitney U -test.

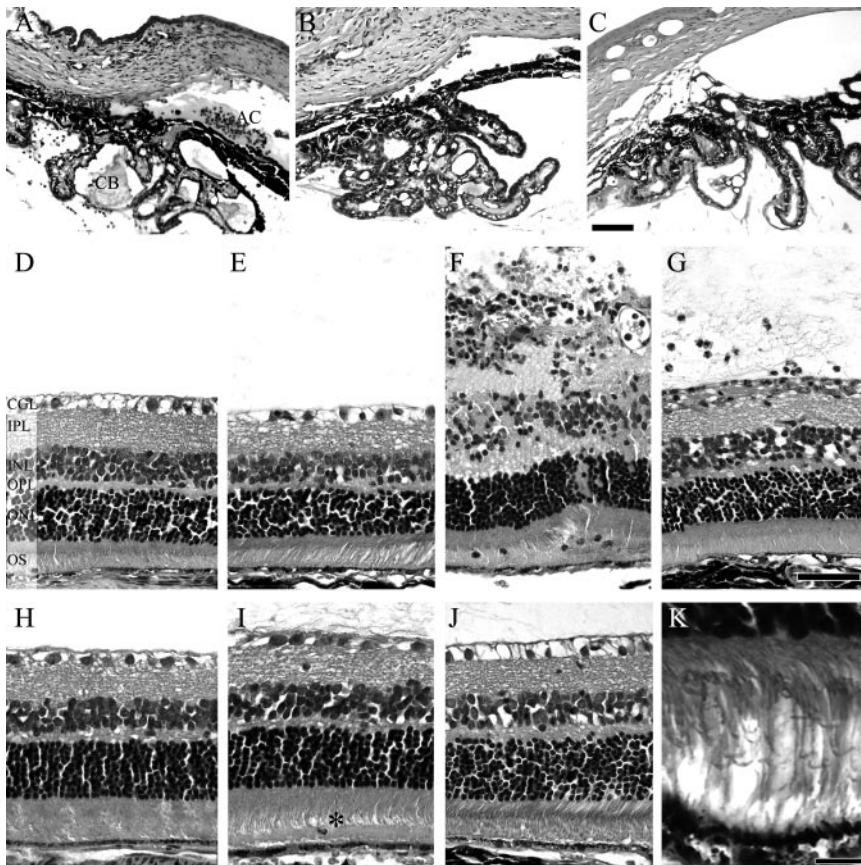


Figure 3. Micrographs of hematoxylin and eosin stained sections of anterior chamber angle and retina, 24 hours or 8 days after vehicle or LPS injection in the presence or absence of melatonin. An intense inflammatory cell infiltration was observed in anterior chamber structures 24 hours after LPS injection (**A**). The treatment with melatonin decreased cell infiltration (**B**). Eight days after LPS injection no signs of inflammation were observed in the anterior chamber angle (**C**). Sections of representative retinas obtained 24 hours after the following treatments: vehicle (**D**), vehicle + melatonin (**E**), LPS (**F**), LPS + melatonin (**G**). Note the altered thickness of retinal layers, focal hemorrhages and cellular infiltration induced by LPS injection (**F**), and the apparently normal morphology in retinas from eyes injected with LPS in the presence of melatonin (**G**). Representative retinas obtained 8 days after the following treatments: vehicle (**H**), LPS (**I**), LPS + melatonin (**J**). No evident morphological differences were appreciated between treatments, except for disorganization of the photoreceptor outer segments observed in eyes injected with LPS (**asterisk**, **I**). This is also shown at high magnification in photograph **K**. Shown are images representative of four different preparations. AC, anterior chamber; CB, ciliary body; GCL, ganglion cell layer; IPL, inner plexiform layer; INL, inner nuclear layer; OPL, outer plexiform layer; ONL, outer nuclear layer; OS, outer segments; scale bar: A–C, K = 30 μ m; D–J = 50 μ m.

To further analyze the inner and outer blood retinal barrier (BRB), a lanthanum tracing analysis was performed. In vehicle-injected eyes, electron dense tracer deposits were observed in blood vessels lumina (data not shown) whereas in LPS-injected eyes, the tracer filling almost the entire length of intercellular junctions of endothelial cells and reaching the basement lamina was frequently observed (Figure 4, A–B). The treatment with melatonin prevented these alterations. In this case, the tracer did not traverse beyond the endothelial cells into the capillary basement lamina of the pericapillary space (Figure 4, C–D). The analysis of the outer BRB, constituted by RPE cell junctions, also revealed differences among experimental groups, as shown in Figure 4. In

retinas from eyes injected with LPS, electron dense deposits were detected in the luminal surface of the choriocapillary layer through the extracellular matrix, both between uveal melanocytes and fibroblasts, as well as filling the Bruch's membrane and the space among microvilli of the RPE basal labyrinth (Figure 4, E–F). In addition, lanthanum deposits were observed in intercellular junctions among RPE cells, penetrating the neural retina (Figure 4G). In animals treated with melatonin, tracer deposits were observed at the luminal surface of the choriocapillary layer capillaries and on the Bruch's membrane, but not between apical prolongations of RPE cells surrounding photoreceptor external segments (Figure 4, H–I). The tracer was frequently observed deeply seeping into the

Table 1. Total Retinal and Retinal Layer Thickness (in μ m)

	24 hours				8 days			
	Vehicle	Melatonin	LPS	LPS + Melatonin	Vehicle	Melatonin	LPS	LPS + Melatonin
Retina	132 \pm 20	137 \pm 26	250 \pm 46**	130 \pm 18 ^a	127 \pm 18	117 \pm 15	152 \pm 29	133 \pm 21
OS	26 \pm 4	27 \pm 10	55 \pm 17**	26 \pm 6 ^a	21 \pm 5	24 \pm 2	40 \pm 23**	24 \pm 5 ^a
ONL	36 \pm 4	36 \pm 8	70 \pm 16**	35 \pm 8 ^a	33 \pm 8	32 \pm 4	39 \pm 6	34 \pm 6
OPL	8 \pm 2	8 \pm 2	21 \pm 6**	8 \pm 2 ^a	10 \pm 4	8 \pm 2	8 \pm 4	8 \pm 2
INL	20 \pm 2	19 \pm 6	40 \pm 12**	17 \pm 6 ^a	22 \pm 3	14 \pm 2	18 \pm 4	22 \pm 5
IPL	25 \pm 6	27 \pm 4	47 \pm 8**	28 \pm 4 ^a	28 \pm 2	22 \pm 2	25 \pm 10	27 \pm 6
GCL	15 \pm 5	13 \pm 3	36 \pm 8**	17 \pm 8 ^a	20 \pm 5	12 \pm 3	12 \pm 5	15 \pm 4

OS, photoreceptor outer segments; ONL, outer nuclear layer; OPL, outer plexiform layer; INL, inner nuclear layer; IPL, inner plexiform layer; GCL, ganglion cell layer. Data are mean \pm SE (n = 4 retinas/group) in μ m. ** P < 0.01 vs. vehicle injected eyes; ^a P < 0.01 vs. LPS-injected eyes by Tukey's test.

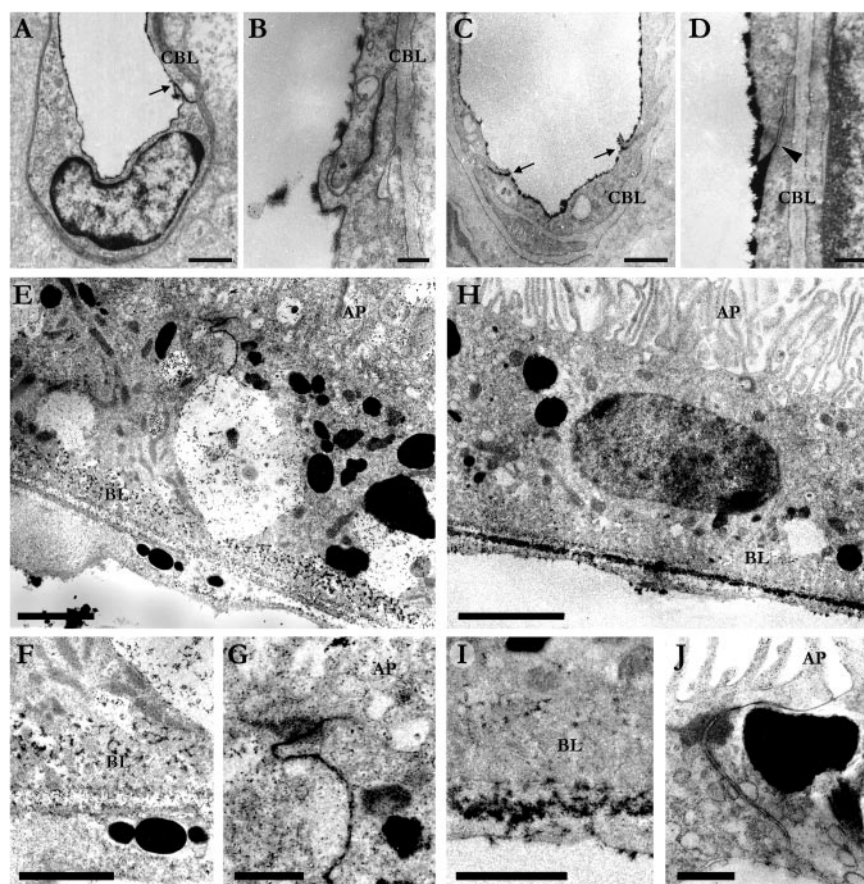


Figure 4. Analysis of the inner (A–D) and outer (E–J) BRB integrity at transmission electron microscopy, 24 hours after LPS injection with or without melatonin. (A): Transverse section of a capillary from LPS-injected eye. Lanthanum was localized on the luminal surface of endothelial cells as well as filling intercellular spaces (arrow, A). At higher magnification, the intercellular space showed a deep penetration of the tracer (B). In eyes injected with LPS from animals treated with melatonin the electron-dense tracer was restricted to the luminal side of tight junctions (arrows, C). Note that the diffusion of the tracer was blocked half way down the intercellular space by an intercellular tight junction (arrowhead, D). In LPS-injected eyes the tracer was mainly localized in cytoplasmic vacuoles (E), in the basal labyrinth (F), and beyond cell junctions of the RPE up to the region of photoreceptor outer segments (G). In eyes injected with LPS from animals treated with melatonin, the tracer was principally arrested by the Bruch's membrane (H). Small amounts of the tracer were observed in the basal labyrinth (I) and in the intercellular space between RPE cells up to tight junctions, but not penetrating the neural retina (J). AP, apical prolongations; CBL, capillary basement lamina; BL, basal labyrinth. Scale bar: A, C, F, G, I, J = 1 μ m; B, D = 0.25 μ m; E = 3 μ m; H = 5 μ m.

RPE interspaces, filling almost the entire length of intercellular junctions, but it was prevented from reaching the neural retina by tight junctions (Figure 4J).

Retinal immunoreactivity for GFAP and vimentin were analyzed at 24 hours and 8 days after the intravitreal injection of vehicle or LPS in animals untreated or treated with melatonin. After 24 hours, the injection of LPS as compared to vehicle induced an increase in retinal GFAP levels (Figure 5, A–B), while after 8 days (Figure 5, D–E) a further increase of this parameter was observed. At both intervals, GFAP immunoreactivity was associated with activated retinal astrocytes and Müller cells. The treatment with melatonin prevented the increase in GFAP immunoreactivity both at 24 hours and 8 days after LPS injection (Figure 5, C and F, respectively). Vimentin immunostaining (Figure 5, G–I) did not change in any of the experimental groups at 24 hours or at 8 days postinjection (data not shown). No significant differences were observed in the density of stained Müller cell processes in any experimental group (data not shown).

At the ultrastructural level, a high disorganization of photoreceptor outer segments was observed in retinas from LPS-injected eyes, with an increased intercellular space filled with membranous debris and macrophages (Figure 6A). In retinas from eyes treated with LPS, altered shapes of photoreceptor outer segment's disks and in some cases, loss of their external membrane, were observed (Figure 6B). Edemas were frequently observed in RPE (Figure 6E). In retinas from eyes injected with LPS in

the presence of melatonin, outer segments (OS) were similar in structure to that observed in retinas from vehicle-injected eyes, eg, stacks of membranous disks relatively well ordered and enclosed in a cell membrane (Figure 6, C–D). In the RPE, phagosomes were regularly observed (Figure 6F).

Figure 7 shows representative scotopic ERG traces recorded 8 days after intravitreal injection of vehicle or LPS in the presence or absence of melatonin, while the average amplitudes of scotopic ERG a- and b-waves are depicted in the right panel of the same Figure. The ERG a- and b-wave amplitude was significantly lower in eyes injected with LPS than in those from eyes injected with vehicle. The presence of melatonin prevented these electroretinographic changes. The ERG a- and b-wave latencies did not change among all of the experimental groups (data not shown). Therefore, the functional analysis also showed that visual function was successfully rescued from retinal damage during inflammation by melatonin.

To get insight into the mechanism of action of melatonin in experimental uveitis, retinal NOS activity and TNF α levels were assessed after 24 hours of vehicle or LPS injection in animals untreated or treated with melatonin. As shown in Figure 8, LPS increased both parameters and melatonin significantly prevented the effect of LPS. Figure 9 shows representative Western blot analysis of nuclear NF κ B p50 and p65 subunit levels in retinas from eyes injected with vehicle or LPS in the presence or absence of melatonin. After 3 hours of injection, LPS

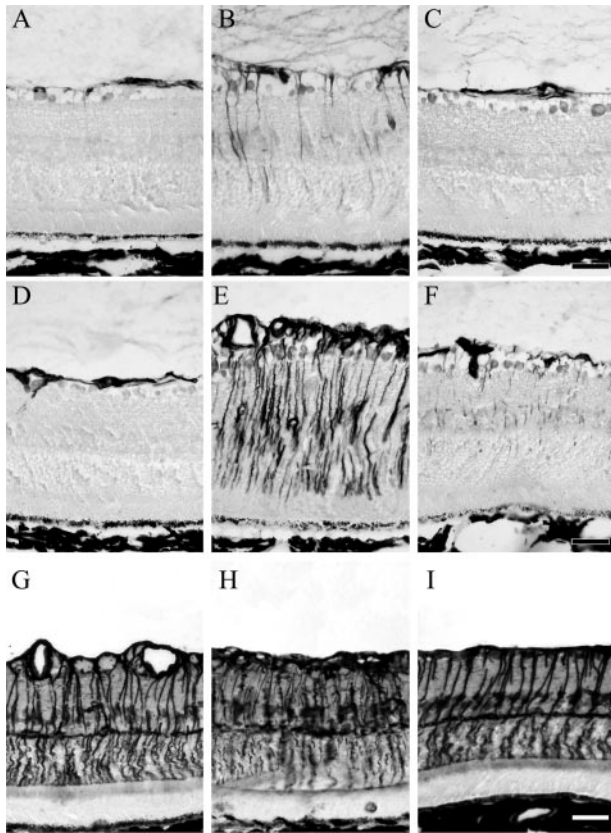


Figure 5. Effect of vehicle or LPS in the presence or absence of melatonin on retinal GFAP and vimentin levels. Upper panel: Immunohistochemistry anti-GFAP 24 hours after the following treatments: vehicle (A), LPS (B), LPS + melatonin (C). Middle panel: Immunohistochemistry for anti-GFAP, 8 days after the following treatments: vehicle (D), LPS (E), LPS + melatonin (F). At both intervals, GFAP-immunoreactivity was observed in astrocytes and Müller cells, throughout the plexiform layer, and outlining angular nuclear profiles in the inner nuclear layer after LPS injection. Melatonin reduced GFAP immunoreactivity at both intervals, showing only few positive Müller cells. Lower panel: Immunohistochemistry anti-vimentin of retinas from vehicle (G), LPS-injected (H) or LPS-injected eyes in the presence of melatonin (I), 24 hours after injections. No differences in vimentin immunoreactivity were observed among groups. Scale bar = 30 μ m.

significantly increased nuclear levels of NF κ B p50 and p65 subunits, while melatonin prevented the effect of LPS.

Retinal melatonin levels were assessed at different intervals after the implantation of the subcutaneous pellet. A significant increase of this parameter ($P < 0.01$) was observed 24 hours but not 8 days after the pellet implantation (eg, control [non-implanted]: 0.21 ± 0.02 , 24 hours after: 0.33 ± 0.03 , and 8 days after: 0.26 ± 0.02 ng melatonin/mg protein; $n = 8$ retinas/group).

Discussion

Uveitis is the most frequent form of intraocular inflammation and is a major cause of visual disability. The present results indicate that melatonin significantly attenuated biochemical, clinical, histological, ultrastructural, and functional alterations induced by experimental uveitis, probably through an NF κ B-dependent mechanism. It was previously shown that melatonin significantly reduces

edematous effects of experimental uveitis in the guinea pig retina.⁴² The present results further support the preventive action of melatonin in experimental uveitis by showing its beneficial effect at different levels.

Experimental models of uveitis were developed in several species by LPS intravenous, intraperitoneal, or footpad administration. In this report, we used an intravitreal injection of the endotoxin since this maneuver avoids systemic inflammations and allows the use of the contralateral eye (which did not show clinical or histological changes in comparison with non-injected eyes [data not shown]) as control, minimizing the number of animals, and decreasing their mortality. As described in other species,^{8,43} the intravitreal injection of LPS in the golden hamster induced several signs of uveitis such as disruption of the BOB, dilatation of conjunctival vessels, iridial hyperemia, and flare in the anterior chamber. In addition to these anterior segment (anterior chamber, iris, and ciliary body) alterations, the examination of the posterior segment showed retinal vasculitis, hemorrhagic exudates, focal destruction of photoreceptors, and retinal infiltration. Clinical and histopathological abnormalities were evident at 24 hours postinjection and were mostly recovered by 8 days. These results support that intravitreal injection of LPS in the hamster evoked a reproducible and characteristic acute inflammatory response that mimics central features of human uveitis.

Melatonin significantly decreased the effect of LPS on protein concentration and cell number in hamster aqueous humor, suggesting that it could contribute to preserve BOB integrity. In agreement, it was shown that melatonin attenuates the postischemic increase in blood-brain barrier permeability following ischemic stroke in mice,⁴⁴ reduces cerebral edema, and decreases blood-brain barrier permeability in rats.⁴⁵ In addition, it was demonstrated that melatonin protects endothelial barrier integrity and preserves microvascular blood perfusion after ischemia reperfusion in hamster cheek pouch.⁴⁶ As we will discuss later, the present report also provides ultrastructural evidence on the effect of the methoxyindole on BOB preservation.

In the presence of melatonin, a significant reduction of clinical signs induced by LPS was observed. This effect was not specific for particular signs, since all were reduced in the presence of melatonin. The decrease in anterior clinical signs correlated with a decrease in anterior segment inflammation. In the presence of melatonin, reduced cell infiltration was observed in the iris, ciliary body, limbus, retina, and vitreous. The BRB is part of the BOB, consisting in cells that are joined tightly together, constituted by non-fenestrated capillaries of the inner retinal circulation and tight-junctions between retinal pigment epithelium cells. The BOB is a barrier created by endothelium of capillaries of the retina, iris, and ciliary epithelium, as well as the retinal pigment epithelium. The results of inner and outer BRB analysis using lanthanum as an ultrastructural tracer showed that in LPS-injected eyes, the tracer filled spaces between adjacent endothelial cells and between photoreceptor outer segments, indicating a breakdown of both BRBs, which was prevented by melatonin. In melatonin-treated eyes, lantha-

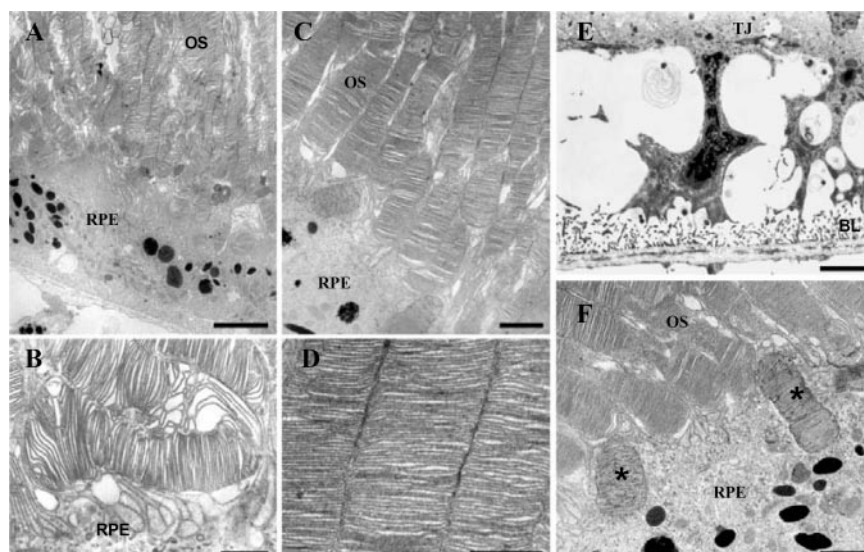


Figure 6. Ultrastructural analysis of photoreceptors from retinas obtained 8 days after LPS injection in the presence or absence of melatonin. LPS injection provoked a high disorganization of photoreceptor outer segments (**A**). At a higher magnification, the space between cells and the altered shape of membranous disks can be observed (**B**). The same retinal region in eyes from animals treated with melatonin showed ultrastructural preservation of photoreceptor outer segments (**C**). At a higher magnification the integrity of the stack of disks is clearly shown (**D**). In LPS-injected eyes, wider intercellular spaces and cytoplasmic edema in some regions of the RPE were observed (**E**). In melatonin-treated animals, the apical region of RPE showed large amounts of phagosomes with ingested disk material (**asterisk**, **F**). Scale bar: A = 5 μ m; B and D = 1 μ m; C, E, and F = 2 μ m. BL, basal labyrinth; OS, outer segments; RPE, retinal pigment epithelium; TJ, tight junction.

num deposits were never observed in the albuminal side of retinal endothelial cells or extending beyond the RPE. It seems likely that in animals treated with melatonin, tight junctions were functional, being capable of preventing extravasations of the tracer through intercellular spaces. This finding is compatible with the observations by Kaur et al³⁶ who demonstrated that melatonin protects the inner BRB in the rat hypoxic retina.

Müller cells play an important role in the maintenance and regulation of the BRB, as they have a close spatial relationship with retinal blood vessels.⁴⁷ GFAP up-regulation is a hallmark of reactive astrocytes⁴⁸ and retinal

pathology modulates its expression.^{49,50} Müller cells that do not express GFAP under physiological conditions are known to express GFAP in pathological situations.^{51,52} The present results indicate that the injection of LPS provoked a significant alteration in retinal Müller cells, as shown by an increase in GFAP immunoreactivity that was prevented by melatonin.

To assess retinal function in experimental uveitis, scotopic flash ERGs were performed in eyes from animals injected with LPS or vehicle, since the hamster has a predominantly rod-retina. A significant reduction of a- and b-wave amplitude, but not their latencies, was observed after 8 days of intravitreal injection of LPS. The fact that ERG alterations were evident at a period in which most of the clinical and histological changes were not evident (8 days), suggests that LPS provoked retinal sequelae that were also prevented by melatonin. Eight days after the injection of LPS, a high disorganization of photoreceptors outer segments persisted. At ultrastructural level, significant alterations of cell architecture were observed with widened intercellular spaces containing dense bodies and membranous debris. These results support a correlation between retinal morphology and electroretinographic activity. The amplitude of the a-wave depends on the integrity of the photoreceptors and on absorption of quanta in photoreceptors, whereas the amplitude of the b-wave depends on that of the a-wave and reflects bipolar and Müller cells function. This way, LPS-induced alterations in photoreceptor morphology could be involved in a-wave changes, while alterations in Müller cells (GFAP up-regulation) might provoke a decrease in the b-wave amplitude. As shown herein, histological alterations induced by LPS were prevented by melatonin, therefore it is not surprising the recovery in ERG induced by the methoxyindole. In addition, in melatonin-treated eyes, large amount of phagosomes were observed in RPE cells, which could indicate an active renovation and repairing of outer segment membranous disks.

There remains to be established the mechanism/s involved in the protection induced by melatonin. It is well

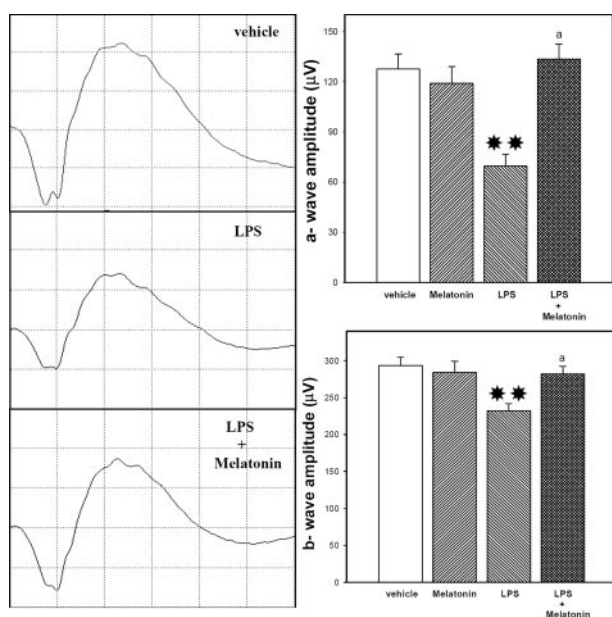


Figure 7. Scotopic ERGs of hamster injected 8 days before with vehicle or LPS in the presence or absence of melatonin. **Left panel:** representative scotopic ERG traces. **Right panel:** average amplitudes of scotopic ERG a- and b-waves. A significant reduction in the amplitude (but not their latencies) of both scotopic ERG a- and b-wave amplitude was observed in eyes injected with LPS, whereas melatonin significantly reduced these ERG alterations. Data are mean \pm SE ($n = 20$ eyes/group). ** $P < 0.01$ vs. vehicle injected eyes; a: $P < 0.01$ vs. LPS-injected eyes by Tukey's test.

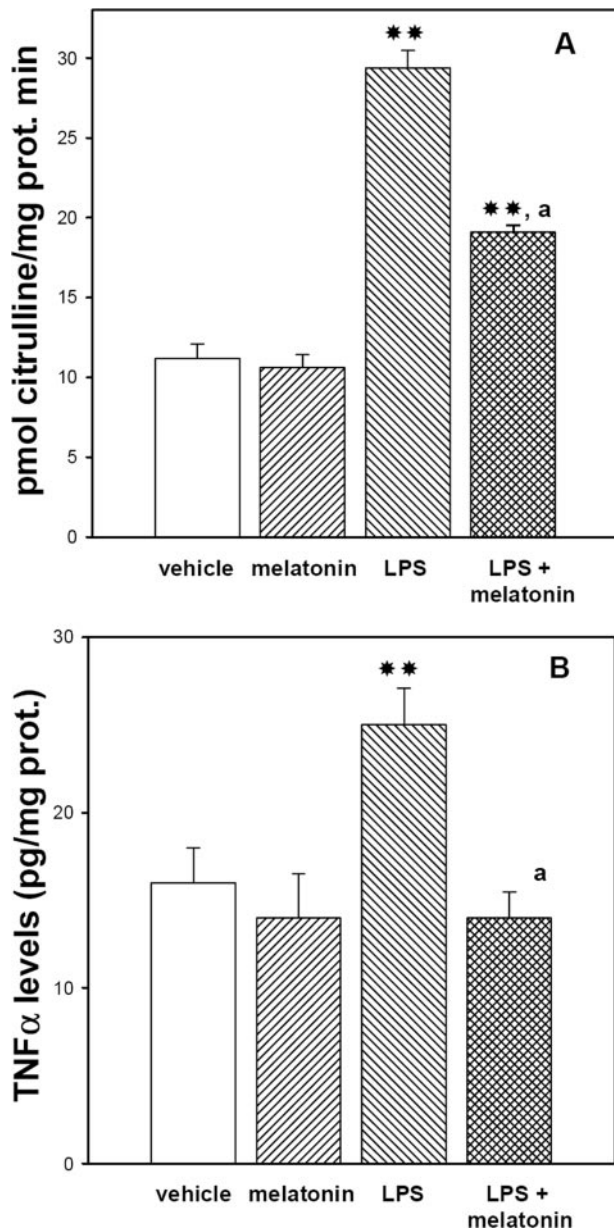


Figure 8. Effect of LPS on retinal NOS activity and TNFα levels. One day after injections, both parameters were significantly higher in LPS- than in vehicle-injected. Melatonin, which was ineffective per se, significantly reduced NOS activity (**panel A**) and TNFα levels (**panel B**) in the retina from LPS-injected eyes. Data are mean ± SE (*n* = 8 retinas/group), ***P* < 0.01 vs. vehicle-injected eyes; a: *P* < 0.01 vs. LPS-injected eyes by Tukey's test.

established that LPS induces iNOS expression as well as a cascade of cytokine synthesis in different systems (for a review see ⁵³). The present results show that melatonin decreased the effect of LPS on two key signals involved in inflammatory processes, such as NOS activity and TNFα levels. NFκB is one of the most important transcription factors in transcriptional regulation of inflammatory proteins.^{54,55} Activated NFκB translocates to the nucleus, where it binds to κB binding sites in the promoter regions of target genes, and induces the transcription of pro-inflammatory mediators, eg, iNOS, TNFα, cyclooxygenase-2, and IL-1b, IL-6, and IL-8.⁵⁶ The fact that melatonin prevented the LPS-induced increase in nuclear levels of

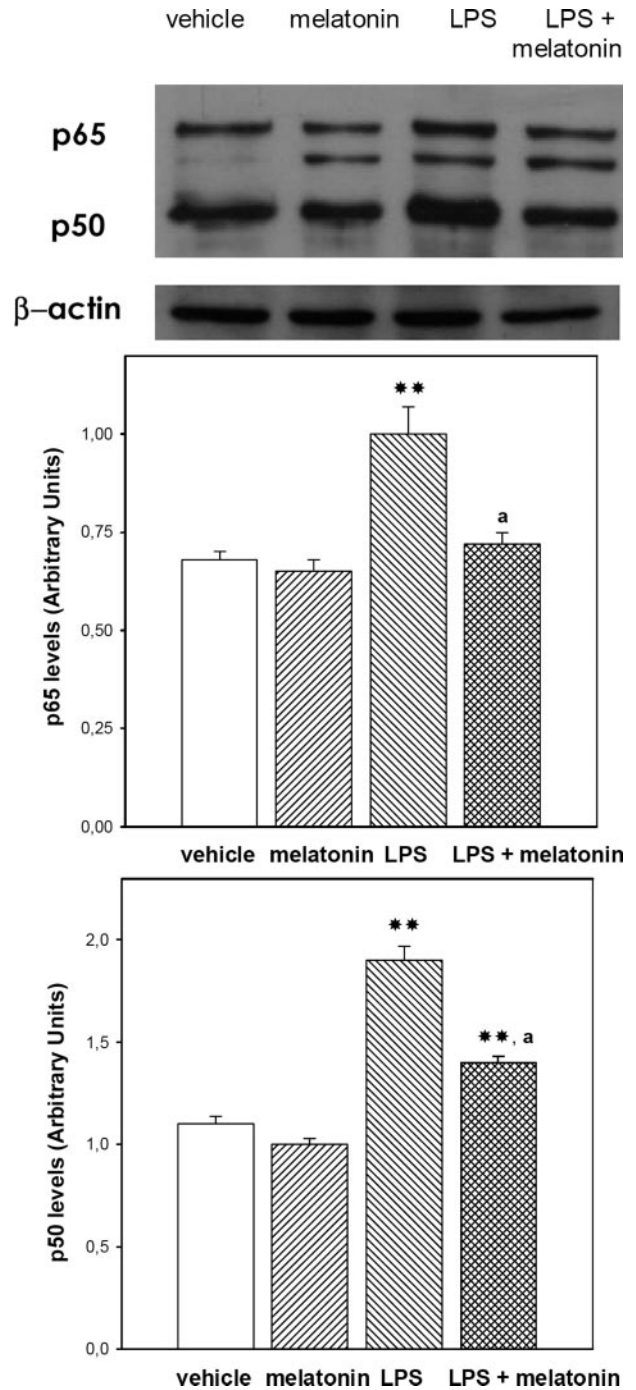


Figure 9. Top panel: Western blot analysis of nuclear NFκB subunits p50 and p65 levels. Each lane was loaded with 50 μg of nuclear proteins, as described in the Material and Methods. Middle, bottom panel: Data are mean ± SEM (*n* = 8 retinas/group) of densitometric values for p50 and p65 levels relative to β-actin band intensity, ***P* < 0.01 vs. vehicle injected eyes; a: *P* < 0.01 vs. LPS-injected eyes, by Tukey's test.

p50 and p65 could account for the decrease in NOS activity and TNFα levels. These results suggest that NFκB could be a main target for the anti-inflammatory effect of melatonin in EIU. In agreement with these results, it was demonstrated that melatonin inhibits iNOS expression by inhibiting the activation of NFκB in immunostimulated murine macrophages,⁵⁷ rat skeletal muscle,⁵⁸ and C6

glioma cells.⁵⁹ Furthermore, it was shown that melatonin reduces colonic inflammatory injury⁶⁰ and carbon tetrachloride-induced hepatic fibrogenesis⁶¹ by down-regulating pro-inflammatory molecules such as TNF α mediated by NF κ B inhibition.⁶⁰

Uveitis, a disease with potentially blinding sequels (synechiae, cataracts, and macular and optic nerve edema, with loss of vision and loss of the eye), remains a challenging field to ophthalmologists, as the disease causes significant morbidity, and the use of traditional forms of treatment is restricted by limited effectiveness and considerable side effects. As mentioned before, ocular inflammation is mainly treated with topical and/or systemic application of corticosteroids. During long-term treatment with corticosteroids, however, care must be taken to guard against both ocular and systemic complications such as cataract, glaucoma, diabetes, hypertension, and osteoporosis. Therefore, the establishment of additive anti-inflammatory approaches is desirable to decrease the rate and degree of these complications. The present results suggest that melatonin, which lacks adverse collateral effects even at high doses, could be a promising resource in the management of uveitis. Alone or combined with corticosteroid therapy, the anti-inflammatory effects melatonin may benefit patients with chronic uveitis and decrease the rate and degree of corticosteroid-induced complications. Although in the present study only the preventive effect of melatonin in experimental uveitis was demonstrated, this "relative weakness" does not preclude its clinical relevance. Indeed, uveitis is a common consequence of ocular surgery (cataract surgery and vitrectomy, among others). Thus, even as preventive strategy, the present results suggest that melatonin, a very safe compound for human use, should be included in the ophthalmic therapeutic resources.

References

- de Vos AF, Klaren VN, Kijlstra A: Expression of multiple cytokines and IL-1RA in the uvea and retina during endotoxin-induced uveitis in the rat. *Invest Ophthalmol Vis Sci* 1994, 35:3873–3883
- Planck SR, Huang XN, Robertson JE, Rosenbaum JT: Cytokine mRNA levels in rat ocular tissues after systemic endotoxin treatment. *Invest Ophthalmol Vis Sci* 1994, 35:924–930
- Bellot JL, Palmero M, Garcia-Cabanes C, Espi R, Hariton C, Orts A: Additive effect of nitric oxide and prostaglandin-E2 synthesis inhibitors in endotoxin-induced uveitis in the rabbit. *Inflamm Res* 1996, 45:203–208
- Rao N: Role of oxygen free radicals in retinal damage associated with experimental uveitis. *Trans Am Ophthalmol Soc* 1990, 88:797–850
- Hashida M, Fukushima A, Zhang J, Kodama H, Ueno H: Involvement of superoxide generated by polymorphonuclear leukocytes in endotoxin-induced uveitis. *Graefes Arch Clin Exp Ophthalmol* 2000, 238:359–365
- Jacquemin E, de Kozak Y, Thillaye B, Courtois Y, Goureau O: Expression of inducible nitric oxide synthase in the eye from endotoxin-induced uveitis rats. *Invest Ophthalmol Vis Sci* 1996, 37:1187–1196
- Bhattacharjee P: Prostaglandins and inflammatory reactions in the eye. *Methods Find Exp Clin Pharmacol* 1980, 2:17–31
- Howes EL Jr., McKay DG: The effects of aspirin and indomethacin on the ocular response to circulating bacterial endotoxin in the rabbit. *Invest Ophthalmol* 1976, 15:648–651
- Goureau O, Bellot J, Thillaye B, Courtois Y, de Kozak Y: Increased nitric oxide production in endotoxin-induced uveitis. Reduction of uveitis by an inhibitor of nitric oxide synthase. *J Immunol* 1995, 154:6518–6523
- Sonoki T, Nagasaki A, Gotoh T, Takiguchi M, Takeya M, Matsuzaki H, Mori M: Coinduction of nitric-oxide synthase and arginase I in cultured rat peritoneal macrophages and rat tissues in vivo by lipopolysaccharide. *J Biol Chem* 1997, 272:3689–3693
- McCluskey PJ, Towler HM, Lightman S: Management of chronic uveitis. *BMJ* 2000, 320:555–558
- Gaudio PA: A review of evidence guiding the use of corticosteroids in the treatment of intraocular inflammation. *Ocul Immunol Inflamm* 2004, 12:169–192
- McGhee CN, Dean S, Danesh-Meyer H: Locally administered ocular corticosteroids: benefits and risks. *Drug Saf* 2002, 25:33–55
- El Afrit MA, Mazlout H, Trojet S, Laguech L, Megaieth K, Belhaj S, Khemiri N, Kraiem A: Cortisone glaucoma: epidemiological, clinical, and therapeutic study. *J Fr Ophtalmol* 2007, 30:49–52
- Cheng HF, Harris RC: Renal effects of non-steroidal anti-inflammatory drugs and selective cyclooxygenase-2 inhibitors. *Curr Pharm Des* 2005, 11:1795–1804
- Vakil N: The prevention of gastropathy and upper abdominal symptoms caused by nonsteroidal anti-inflammatory drugs. *Rev Gastroenterol Disord* 2006, 6:221–226
- Rosenbaum JT, McDevitt HO, Guss RB, Egbert PR: Endotoxin-induced uveitis in rats as a model for human disease. *Nature* 1980, 286:611–613
- Nathan C, Xie QW: Nitric oxide synthases: roles, tolls, and controls. *Cell* 1994, 78:915–918
- Miyamoto K, Ogura Y, Hamada M, Nishiwaki H, Hiroshiba N, Honda Y: In vivo quantification of leukocyte behavior in the retina during endotoxin-induced uveitis. *Invest Ophthalmol Vis Sci* 1996, 37:2708–2715
- Pang SF, Lee PP, Tang PL: Sensory receptors as a special class of hormonal cells. *Neuroendocrinology* 1991, 53 Suppl 1:2–11
- Faillace MP, Sarmiento MI, Rosenstein RE: Melatonin effect on [³H] glutamate uptake and release in the golden hamster retina. *J Neurochem* 1996, 67:623–628
- Tosini G, Fukuhara C: Photocircadian regulation of retinal melatonin in mammals. *J Neuroendocrinol* 2003, 15:364–369
- Faillace MP, Cutrera R, Sarmiento MI, Rosenstein RE: Evidence for local synthesis of melatonin in golden hamster retina. *Neuroreport* 1995, 6:2093–2095
- Huether G: The contribution of extrapineal sites of melatonin synthesis to circulating melatonin levels in higher vertebrates. *Experientia* 1993, 49:665–670
- Hardeland R, Pandi-Perumal SR, Cardinali DP: Melatonin. *Int J Biochem Cell Biol* 2006, 38:313–316
- Allegra M, Reiter RJ, Tan DX, Gentile C, Tesoriere L, Livrea MA: The chemistry of melatonin's interaction with reactive species. *J Pineal Res* 2003, 34:1–10
- Rodriguez C, Mayo JC, Sainz RM, Antolin I, Herrera F, Martín V, Reiter RJ: Regulation of antioxidant enzymes: a significant role for melatonin. *J Pineal Res* 2004, 36:1–9
- Tan DX, Manchester LC, Terron MP, Flores LJ, Reiter RJ: One molecule, many derivatives: a never-ending interaction of melatonin with reactive oxygen and nitrogen species? *J Pineal Res* 2007, 42:28–42
- Manda K, Ueno M, Anzai K: AFMK, a melatonin metabolite, attenuates X-ray-induced oxidative damage to DNA, proteins and lipids in mice. *J Pineal Res* 2007, 42:386–393
- Siu AW, Maldonado M, Sanchez-Hidalgo M, Tan DX, Reiter RJ: Protective effects of melatonin in experimental free radical-related ocular diseases. *J Pineal Res* 2006, 40:101–109
- Benítez-King G: Melatonin as a cytoskeletal modulator: implications for cell physiology and disease. *J Pineal Res* 2006, 40:1–9
- Huerto-Delgadillo L, Anton-Tay F, Benítez-King G: Effects of melatonin in microtubule assembly dependent on hormone concentration: role of melatonin as a calmodulin antagonist. *J Pineal Res* 1994, 17:55–62
- Pappolla MA, Sos M, Omar RA, Bick RJ, Hickson-Bick DLM, Reiter RJ, Efthimiopoulos S, Robakis NK: Melatonin prevents death of neuroblastoma cells exposed to the Alzheimer amyloid peptide. *J Neurosci* 1997, 17:1683–1690
- Sáenz DA, Turjanski AG, Sacca GB, Marti M, Doctorovich F, Sarmiento MI, Estrin DA, Rosenstein RE: Physiological concentrations of melatonin

- inhibit the nitridergic pathway in the Syrian hamster retina. *J Pineal Res* 2002, 33:31–36
35. León J, Escames G, Rodríguez MI, López LC, Tapias V, Entrena A, Camacho E, Carrión MD, Gallo MA, Espinosa A, Tan DX, Reiter RJ, Acuña-Castroviejo D: Inhibition of neuronal nitric oxide synthase activity by N1-acetyl-5-methoxykynuramine, a brain metabolite of melatonin. *J Neurochem* 2006, 98:2023–2033
36. Kaur C, Sivakumar V, Yong Z, Lu J, Foulds WS, Ling EA: Blood-retinal barrier disruption and ultrastructural changes in the hypoxic retina in adult rats: the beneficial effect of melatonin administration. *J Pathol* 2007, 212:429–439
37. Lissoni P, Rovelli F, Malugani F, Bucovec R, Conti A, Maestroni GJ: Anti-angiogenic activity of melatonin in advanced cancer patients. *Neuro Endocrinol Lett* 2001, 22:45–47
38. Sáenz DA, Goldin AP, Minces L, Chianelli M, Sarmiento MI, Rosenstein RE: Effect of melatonin on the retinal glutamate/glutamine cycle in the golden hamster retina. *FASEB J* 2004, 18:1912–1913
39. Lowry OH, Rosebrough NJ, Farr AL, Randall RJ: Protein measurement with the Folin Phenol reagent. *J Biol Chem* 1951, 193:265–275
40. DePace DM: Distribution of intravascularly injected lanthanum ions in ganglia of the autonomic nervous system of the rat. *J Auton Nerv Syst* 1984, 11:339–347
41. Jaliffa CO, Howard S, Hoijman E, Salido E, Sarmiento MI, Arias P, Rosenstein RE: Effect of neurosteroids on the retinal gabaergic system and electroretinographic activity in the golden hamster. *J Neurochem* 2005, 94:1666–1675
42. Kukner A, Colakoglu N, Serin D, Alagoz G, Celebi S, Kukner AS: Effects of intraperitoneal vitamin E, melatonin and aprotinin on leptin expression in the guinea pig eye during experimental uveitis. *Acta Ophthalmol Scand* 2006, 84:54–61
43. Koga T, Koshiyama Y, Gotoh T, Yonemura N, Hirata A, Tanihara H, Negi A, Mori M: Coinduction of nitric oxide synthase and arginine metabolic enzymes in endotoxin-induced uveitis rats. *Exp Eye Res* 2002, 75:659–667
44. Chen HY, Chen TY, Lee MY, Chen ST, Hsu YS, Kuo YL, Chang GL, Wu TS, Lee EJ: Melatonin decreases neurovascular oxidative/nitrosative damage and protects against early increases in the blood-brain barrier permeability after transient focal cerebral ischemia in mice. *J Pineal Res* 2006, 41:175–182
45. Gorgulu A, Palaoglu S, Ismailoglu O, Tuncel M, Surucu MT, Erbil M, Killinc K: Effect of melatonin on cerebral edema in rats. *Neurosurgery* 2001, 49:1434–1441
46. Bertuglia S, Marchiafava PL, Colantuoni A: Melatonin prevents ischemia reperfusion injury in hamster cheek pouch microcirculation. *Cardiovasc Res* 1996, 31:947–952
47. Distler C, Dreher Z: Glia cells of the monkey retina - II. Müller cells. *Vision Res* 1996, 36:2381–2394
48. Pekny M, Nilsson M: Astrocyte activation and reactive gliosis. *Glia* 2005, 50:427–434
49. Bignami A, Dahl D: The radial glia of Müller in the rat retina and their response to injury: an immunofluorescence study with antibodies to the glia fibrillary acidic (GFA) protein. *Exp Eye Res* 1979, 28:63–69
50. Wu KH, Madigan MC, Billson FA, Penfold PL: Differential expression of GFAP in early vs. late AMD: a quantitative analysis. *Br J Ophthalmol* 2003, 87:1159–1166
51. Erickson PA, Fisher SK, Guerin CJ, Anderson DH, Kaska DD: Glial fibrillary acidic protein increases in Müller cells after retinal detachment. *Exp Eye Res* 1987, 44:37–48
52. Osborne NN, Block F, Sontag KH: Reduction in ocular blood flow results in glial fibrillary acidic protein (GFAP) expression in rat Müller cells. *Vis Neurosci* 1991, 7:637–639
53. Murphy K, Haudek SB, Thompson M, Giroir BP: Molecular biology of septic shock. *New Horiz* 1998, 6:181–193
54. Xie QW, Kashiwabara Y, Nathan C: Role of transcription factor NF- κ B/Rel in induction of nitric oxide synthase. *J Biol Chem* 1994, 269:4705–4708
55. Ghosh S, May MJ, Kopp EB: NF-kappa B and Rel proteins: evolutionarily conserved mediators of immune responses. *Annu Rev Immunol* 1998, 16:225–260
56. Griscavage JM, Wilk S, Ignarro LJ: Inhibitors of the proteasome pathway interfere with induction of nitric oxide synthase in macrophages by blocking activation of transcription factor NF- κ B. *Proc Natl Acad Sci USA* 1996, 93:3308–3312
57. Gilad E, Wong HR, Zingarelli B, Virág L, O'Connor M, Salzman AL, Szabó C: Melatonin inhibits expression of the inducible isoform of nitric oxide synthase in murine macrophages: role of inhibition of NFkappaB activation. *FASEB J* 1998, 12:685–93
58. Alonso M, Collado PS, González-Gallego J: Melatonin inhibits the expression of the inducible isoform of nitric oxide synthase and nuclear factor kappa B activation in rat skeletal muscle. *J Pineal Res* 2006, 41:8–14
59. Esposito E, Iacono A, Muià C, Crisafulli C, Mattace Raso G, Bramanti P, Meli R, Cuzzocrea S: Signal transduction pathways involved in protective effects of melatonin in C6 glioma cells. *J Pineal Res* 2008, 44:78–87
60. Li JH, Yu JP, Yu HG, Xu XM, Yu LL, Liu J, Luo HS: Melatonin reduces inflammatory injury through inhibiting NF-kappaB activation in rats with colitis. *Mediators Inflamm* 2005, 4:185–93
61. Wang H, Wei W, Wang NP, Gui SY, Wu L, Sun WY, Xu SY: Melatonin ameliorates carbon tetrachloride-induced hepatic fibrogenesis in rats via inhibition of oxidative stress. *Life Sci* 2005, 77:1902–15